Photophysics of Ruthenium Complexes Bound to Double Helical DNA

Challa V. Kumar, Jacqueline K. Barton,* and Nicholas J. Turro*

Contribution from the Department of Chemistry, Columbia University,
New York, New York 10027. Received February 1, 1985

Abstract: Binding of the chiral metal complexes [Ru(bpy)$_3$]Cl$_2$ (I), [Ru(phen)$_3$]Cl$_2$ (II), and [Ru(DIP)$_3$]Cl$_2$ (III) to calf thymus DNA is examined by following changes in the photophysical properties of these probes with use of steady-state as well as time-resolved methods. Increasing luminescence is seen for the ruthenium complexes II and III with DNA addition whereas no enhanced luminescence is detectable for I. A biexponential decay in luminescence is found for II and III with emission lifetimes of the complexes bound to DNA appearing 3–5 times longer than those of the free complexes. Quenching of the luminescence by the ferrocyanide anion further amplifies the ability to distinguish bound forms. I* is quenched by ferrocyanide in the presence of DNA as efficiently as in its absence, indicating little or no binding. In contrast, biphasic Stern–Volmer plots are found for II and III, indicating extensive protection of II* and III* in the presence of DNA from ferrocyanide. Here emission quenching was found to be completely static as a result of counterion condensation at the DNA polyanion. Emission polarization measurements revealed that the binding of II and III to DNA is accompanied by significant increases in the steady-state polarization. The results are interpreted in terms of two binding modes: electrostatic, which is easily quenched by ferrocyanide and contributes no polarization in emission, and intercalative, which is protected from ferrocyanide quenching and, since rigidly bound, retains emission polarization. The distinction becomes more apparent for III where significant enantiomeric selectivity is observed on binding to DNA. Thus Δ-Ru(DIP)$_3{}^{2+}$ binds to DNA both electrostatically and by intercalation; extensive curvature is seen in Stern–Volmer plots, and increases in polarization are observed. The Λ isomer, which gives strictly linear Stern–Volmer plots, binds only electrostatically. This chiral discrimination for intercalative binding is explained in terms of the helical asymmetry of a right-handed DNA structure which is matched by the asymmetry of the Δ isomer but precludes binding by the Λ isomer.

The nature and dynamics of binding small molecules to biopolymers represents an area of active investigation. Studies directed toward the design of site- and conformation-specific reagents provide routes toward rational drug design as well as a means to develop sensitive chemical probes of polymer structure. A simple example is given by the intercalation of small heterocyclic dyes into DNA.[1-4] This noncovalent binding mode where the dye stacks between adjacent base pairs of the DNA duplex is particularly favored by positively charged species possessing a planar aromatic moiety. Intercalators tend to be strongly mutagenic and some have shown promising chemotherapeutic activity.[5] Their carcinogenecity and antitumor activity furthermore correlate well with DNA binding affinity. Moreover, the photophysical properties of bound intercalators have provided useful information concerning nucleic acid structure. Ethidium is a common fluorescence probe for DNA and has recently been employed in examinations of the torsional rigidity of the double helix.[6]

Cationic metal complexes possessing planar aromatic ligands also may bind to DNA by intercalation.[7] Platinum complexes have been shown by X-ray diffraction methods to be valuable electron-dense probes of the intercalative process and generally of nucleic acid structure.[8-10] Metallointercalators which cleave DNA,[11] owing to the redox activity of the metal center, have furthermore been successfully employed in footprinting studies of drug binding and in the examination of higher-order chromatin structure.[12,13]

Chiral octahedral metal complexes containing aromatic ligands have been found recently to display enantiomeric selectivity in binding to double helical DNA.[14] Equilibrium dialysis of DNA with the racemic mixture of chiral metal complexes showed the optical enrichment of the less favored isomer in the dialysate. Absolute configuration assignments for tris(phenanthroline)ruthenium(II) complexes revealed that it is the Δ isomer that binds preferentially to right-handed B-DNA.[15] Ruthenium(II) complexes have been particularly useful in monitoring stereoselective binding to DNA not only because of the stability of enantiomers but also because of the sensitivity of their photophysical properties to DNA binding.[15] Luminescence enhancements and absorption hypochromism in the intense metal to ligand charge transfer band

(MLCT) accompany DNA binding. Furthermore, enantiomers of tris(diphenylphenanthroline)ruthenium(II) have been shown to be useful chemical probes for helix handedness, since absorption decreases accompany binding of the Δ isomer but not of the Λ isomer to a right-handed helix, whereas spectrophotometric titrations indicate that both isomers bind equally to Z-form poly dGC.[16]

In this report a detailed study of the photophysical properties of ruthenium(II) complexes in the presence of DNA has been carried out. We were interested in determining how spectroscopic characteristics of the ruthenium(II) complexes vary as a function of DNA binding, whether different modes of DNA binding might be distinguished by using these photophysical properties, and how best to detect chiral discrimination so as to optimize the sensitivity and utility of our spectroscopic probes for DNA handedness. The relatively long lifetimes of these complexes, their excellent, readily

(1) Berman, M. H.; Young, P. R. *Annu. Rev. Biophys. Bioeng.* **1981,** *10,* 87.

(2) Gale, E. F.; Cundliffe, E.; Reynolds, P. E.; Richmond, M. H.; Waring, M. "The Molecular Basis of Antibiotic Action"; Wiley: London, 1972; p 173.

(3) Waring, M. *J. Mol. Biol.* **1970,** *54,* 247.

(4) Lerman, L. S. *J. Mol. Biol.* **1961,** *3,* 18.

(5) Neidle, S. *Prog. Med. Chem.* **1979,** *16,* 151.

(6) (a) Le Pecq, J. B.; Paoletti, C. *J. Mol. Biol.* **1967,** *27,* 87. (b) Le Pecq, J. B.; Paoletti, C. *Ibid.* **1967,** *27,* 2080.

(7) Lippard, S. J. *Acc. Chem. Res.* **1978,** *11,* 211.

(8) Lippard, S. J.; Bond, P. J.; Wu, K. C.; Bauer, W. R. *Science* **1976,** *194,* 726.

(9) Wang, A. H.; Nathans, J.; van der Marcel, G.; van Boom, J. H.; Rich, A. *Nature (London)* **1978,** *276,* 471.

(10) Wang, Y. S.; Lippard, S. J. *J. Chem. Soc., Chem. Commun.* **1977,** 824.

(11) Barton, J. K. *Comments Inorg. Chem.* **1985,** *3,* 321.

(12) (a) Hertzberg, R. P.; Dervan, P. B. *J. Am. Chem. Soc.* **1982,** *104,* 313. (b) Van Dyke, M. W.; Hertzberg, R. P.; Dervan, P. B. *Proc. Natl. Acad. Sci. U.S.A.* **1982,** *79,* 5470. (c) Van Dyke, M. W.; Dervan, P. B. *Biochemistry* **1983,** *22,* 2373.

(13) (a) Reich, K. A.; Marshall, L. E.; Graham, D. R.; Sigman, D. S. *J. Am. Chem. Soc.* **1981,** *103,* 3582. (b) Pope, L. E.; Sigman, D. S. *Proc. Natl. Acad. Sci. U.S.A.* **1984,** *81,* 3. (c) Cartwright, I. L.; Elgin, S. C. R. *Nucl. Acids. Res.* **1982,** *10,* 5835.

(14) (a) Barton, J. K.; Dannenberg, J. J.; Raphael, A. L. *J. Am. Chem. Soc.* **1982,** *104,* 4967. (b) Barton, J. K. *J. Biomol. Struct. Dyn.* **1983,** *1,* 621.

(15) Barton, J. K.; Danishefsky, A. T.; Goldberg, J. M. *J. Am. Chem. Soc.* **1984,** *106,* 2172.

(16) Barton, J. K.; Basile, L. A.; Danishefsky, A. T.; Alexandrescu, A. *Proc. Natl. Acad. Sci. U.S.A.* **1984,** *81,* 1961.
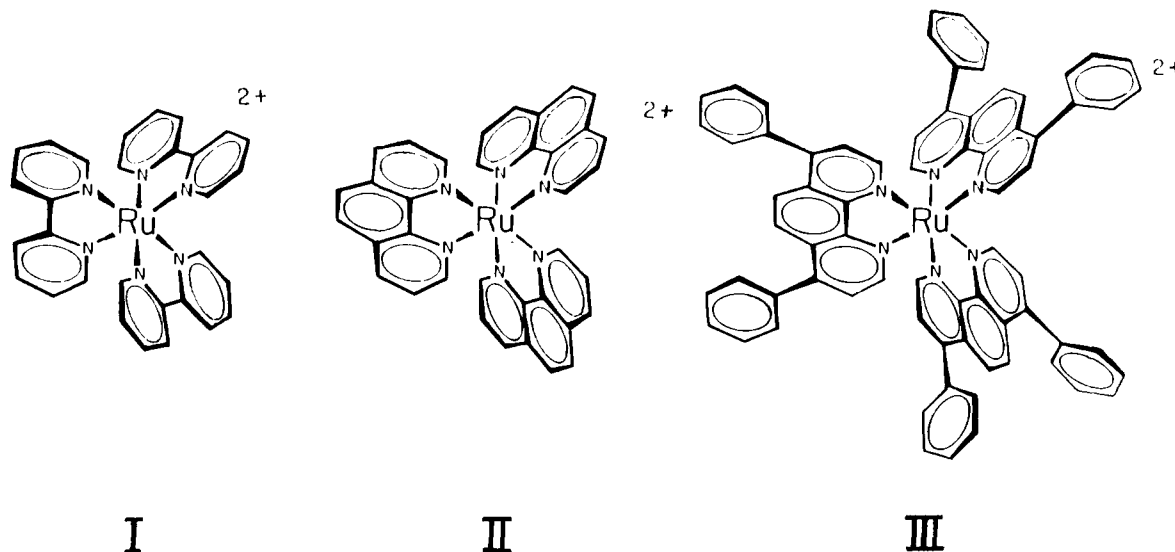
---

* To whom reprint requests should be sent.

Figure 1. The ruthenium complexes (left to right) $Ru(bpy)_3^{2+}$, $Ru(phen)_3^{2+}$, and $Ru(DIP)_3^{2+}$.

measured emission properties in fluid solutions at room temperature, and the inert character of these asymmetric complexes make them ideal candidates for photophysical investigations. The metal complexes employed in the present study are shown in Figure 1 and are denoted respectively as I ($Ru(bpy)_3^{2+}$, bpy = 2,2'-bipyridine), II ($Ru(phen)_3^{2+}$, phen = 1,10-phenanthroline), and III ($Ru(DIP)_3^{2+}$, DIP = 4,7-diphenyl-1,10-phenanthroline).

Experimental Section

Chemicals. Tris(bipyridyl)ruthenium(II) dichloride was purchased from Aldrich and was recrystallized before use. Complexes II and III were prepared by reported procedures.[17] The optical isomers of II and III were separated by using the antimonyl D-tartrate anion as a resolution reagent.[18] Enantiomeric purities, determined on the basis of NMR studies with lanthanide shift reagents,[19] were as follows: Δ-$Ru(DIP)_3^{2+}$, 92% Δ isomer; Λ-$Ru(DIP)_3^{2+}$, >98% optically pure. Experiments were carried out at pH 7.2 by employing buffer 1 (5 mM Tris, 50 mM NaCl) for I and II and buffer 2 (4.5 mM Tris, pH 7.2, 45 mM NaCl, 10% Me_2SO) for III. Concentrations of I and II were typically 10 μM whereas 2.5 μM solutions of III were employed in all the photophysical experiments. All solutions were prepared by using distilled deionized water.

Nucleic Acids. Calf thymus DNA, obtained from Sigma Chemical Co., was purified by phenol extraction as described previously.[20] DNA concentrations per nucleotide were determined spectrophotometrically by employing an extinction coefficient of 6600 M^{-1} cm^{-1} at 260 nm.[21]

Spectrophotometric Measurements. Steady-state luminescence measurements were made on an SLM-4800 spectrometer interfaced with an Apple II computer. Steady-state polarization measurements were made by employing a "T" shaped geometry with Glan-Thompson calcite prism polarizers for excitation and emission monitoring. Lifetime measurements were made by employing a PRA single photon counting unit interfaced with a Hewlett-Packard personal computer. Biexponential traces were analyzed by software written by Dr. C. Doubleday. Time-resolved absorption measurements were made by a nanosecond laser flash photolysis unit described elsewhere.[22] In the latter studies, samples were excited with a Lambda Physik excimer laser (308 nm, 20 ns, 50 mJ) in a perpendicular direction to the monitoring light.

Results and Discussion

General Photophysical Properties. The photophysical properties of the complexes I, II, and III have been measured under various experimental conditions in the presence and absence of nucleic acids. The luminescence spectra of II and III in water under air
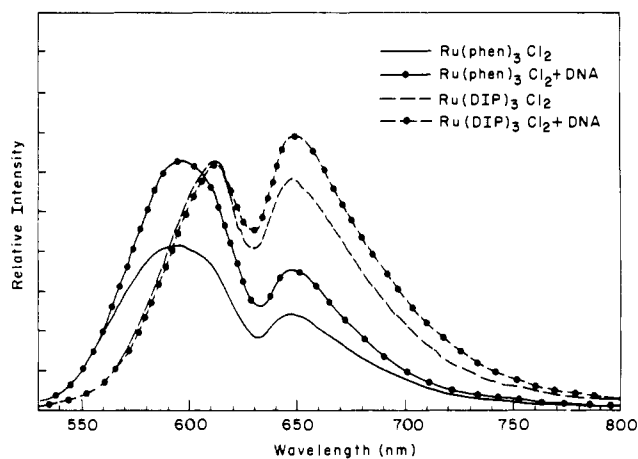
(17) Lin, C.-T.; Bottcher, W.; Chou, M.; Creutz, C.; Sutin, N. *J. Am. Chem. Soc.* **1976**, *98*, 6536.
(18) Gillard, R. D.; Hill, R. E. E. *J. Chem. Soc., Dalton Trans.* **1974**, 1217.
(19) Barton, J. K.; Nowick, J. *J. Chem. Soc., Chem. Commun.* **1984**, 1650.
(20) Barton, J. K.; Lippard, S. J. *Biochemistry* **1979**, *12*, 2661.
(21) Reichmann, M. E.; Rice, S. A.; Thomas, C. A.; Doty, P. *J. Am. Chem. Soc.* **1954**, *76*, 3047.
(22) Turro, N. J.; Aikawa, A.; Butcher, J. A. *J. Quantum Electronics IEEE* **1980**, *QE16*, 1218.

Figure 2. Emission spectra of $Ru(phen)_3^{2+}$ and $Ru(DIP)_3^{2+}$ in the absence and presence of B-form calf thymus DNA.

Table I. General Photophysical Properties of I, II, and III in Air-Saturated Solutions

probe	τ(ns) H_2O	τ(ns) buffer	ϕ_{em} (rel)	λ_{em} H_2O (nm)	k_q-$(K_4Fe(CN)_6)$ $\times 10^{-9} M^{-1} s^{-1}$ H_2O	k_q-$(K_4Fe(CN)_6)$ $\times 10^{-9} M^{-1} s^{-1}$ buffer
I	385	406	0.64	610, 645	34.0	9.0
II	421	525	0.85	596, 645	34.5	8.4
III	909	925	1.00	614, 645	14.5	3.0

saturation are shown in Figure 2 and are not corrected for photomultiplier tube response over the wavelength range shown. The emission from these complexes decays with first-order kinetics at room temperature as monitored by both single photon counting methods as well as by monitoring the emission employing the laser flash photolysis method. These experimental lifetimes are summarized in Table I. Furthermore, the triplet-triplet absorption decay rates, as measured by laser flash photolysis experiments, agreed well with the luminescence decay rates. Slight increases in lifetimes were noticeable from Table I, on going from water to solutions containing 45–50 mM NaCl. The emission from these complexes which is efficiently quenched by oxygen and potassium ferrocyanide (Table I) is assigned as phosphorescence from the MLCT excited state, in accordance with earlier studies.[23] The

(23) (a) Demas, J. N.; Crosby, G. A. *J. Mol. Spectrosc.* **1968**, *26*, 72. (b) Harrigan, R. W.; Crosby, G. A. *J. Chem. Phys.* **1973**, *59*, 3468. (c) Harrigan, R. W.; Hager, G. D.; Crosby, G. A. *Chem. Phys. Lett.* **1973**, *21*, 487.
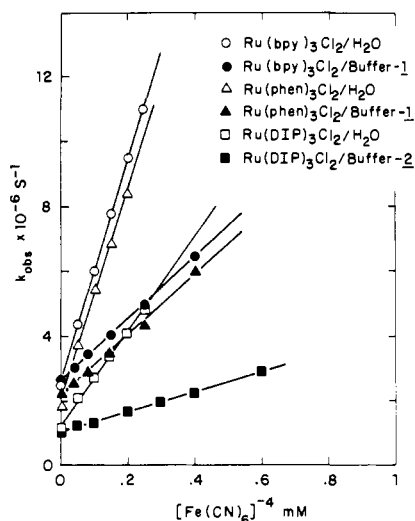
Figure 3. Quenching of emission from ruthenium complexes in water and buffer solutions by potassium ferrocyanide.

Figure 4. Changes in emission intensities for $Ru(bpy)_3^{2+}$, $Ru(phen)_3^{2+}$, and $Ru(DIP)_3^{2+}$ at 614, 596, and 644 nm, respectively, in the presence of B-form calf thymus DNA in buffer solutions.

formal quenching rate constants with potassium ferrocyanide in water are somewhat greater than those expected for diffusional quenching and need some explanation.[24-26] Firstly, these rate constants are evaluated by measuring the emission lifetimes of I, II, and III in the presence of various concentrations of the quencher and therefore represent the dynamic rate constants. Secondly, the decay traces could be adequately fit to a single exponential decay. The quenching rate constants, k_q, were evaluated by using eq 1 where k_d is the rate of decay in the absence of the quencher and [Q] is the concentration of the quencher.

$$k_{obsd} = k_d + k_q[Q] \qquad (1)$$

Linear plots were obtained when k_{obsd} was plotted against the quencher concentration as shown in Figure 3 for I, II, and III.

These large dynamic rate constants can be explained in terms of higher diffusion controlled rates for oppositely charged quencher and quenchee species. These diffusion rates can be calculated by employing the Debye equation[27]

$$k_{diff} = 8NkT/3000\eta b(e^b - 1)^{-1} \qquad (2)$$

where $b = Z_D Z_Q E^2/rtkT$, η is the viscosity of the medium, Z_D and Z_Q are the ionic charges of the donor and quencher, E is the charge of electron, r is the encounter distance between the donor and the quencher, and t is the dielectric constant of the medium. The k_{diff} thus obtained for ferrocyanide and ruthenium dications, with $r = 10$ Å in water, is 42.6×10^9 M^{-1} s^{-1}. The observed values in Table I for I and II are close to this value. Further, the rate constants measured in buffer solutions are lower than in water, and this result is consistent with a reduction in k_q due to increased ionic strength.[28] It may be mentioned that the rate constants obtained by steady-state intensity measurements are consistently greater than the corresponding values given in Table I. This difference can be easily understood in terms of the contributions from static quenching in steady-state experiments. The quenching rate constants for I and II are much larger than those for III, a result that is consistent with the relative sizes of I, II, and III, based on eq 2.

Steady-State Luminescence Studies. Changes in the absorption and emission properties of the Ru(II) probes bound to DNA have
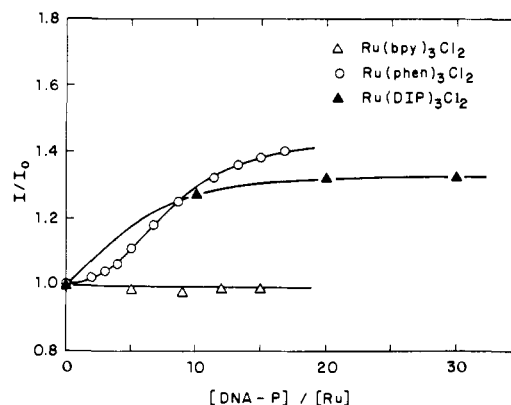
been reported earlier.[15,16] For example, the ground-state absorption spectra of II and III are marginally red shifted upon binding to DNA, with isosbestic points at 464 and 482 nm, respectively. Complexes II and III show marked increases in emission intensities upon binding to DNA, and these spectra have been shown in Figure 2. Curiously, the high and low energy emission bands for II shows increases with binding whereas for III only the band centered at 644 nm is increased.[29] No increase in emission intensity was observed for I in the presence of DNA. Changes in emission intensities for I, II, and III have been plotted against the added DNA–phosphate concentration per mole ruthenium complex in Figure 4. Note that it is the binding characteristics of the excited-state ruthenium complex that are monitored here. In this report, however, for the purposes of discussion it will be assumed that the excited-state binding characteristics qualitatively match that of the ground-state complex. The changes in emission intensities for II and III are marked and reach a plateau region at an ca. 1:20 ratio of ruthenium to DNA–phosphate. This variation in intensity with DNA addition provides direct evidence for a strong interaction between the positively charged ruthenium complexes II and III and the DNA polymer. The observation of little or no change in emission intensities for I is best attributed to a low intrinsic binding constant to DNA of this metal complex. Further since no emission increases are seen with I even with high concentrations of DNA present, it is clear that changes in solution viscosity with DNA addition cannot account for the emission enhancements seen for II and III. The photophysical characteristics of I with DNA then serve as a valuable control for the experiments below.

The increase in emission intensities for II and III upon binding to DNA is due largely to the change in the environment of the metal complex. Although the photophysical properties of the ruthenium complexes are found to be solvent insensitive,[30] a strong isotope effect in water has been observed for I and III.[31] Thus in the case of III, the alteration in water structure around the metal complex as a function of binding may dominate the fluctuations in emission intensities observed. Hydrophobic interactions between the ligands and the nucleic acid bases may also induce changes in the excited-state properties, since it is found that complexes with increased ligand hydrophobicities show greater increases in emission intensities upon binding to polyelectrolytes.[31] It is interesting to note that even the electrostatic association (vide infra) yields an increase in emission intensity, thus the decrease in vibrational modes of relaxation as a result of intercalative binding can account only in part for the luminescence changes observed.

Further support for the binding of II and III to DNA is obtained through steady-state emission quenching experiments. A highly

(24) Juris, A.; Gandolfi, M. T.; Manfrin, M. F.; Balzani, V. *J. Am. Chem. Soc.* **1976**, *98*, 1047.

(25) Juris, A.; Manfrin, M. F.; Masetin, M.; Serpone, N. *Inorg. Chem.* **1978**, *17*, 2258.

(26) Toma, H. E.; Creutz, C. *Inorg. Chem.* **1977**, *16*, 545.

(27) Debye, P. *Trans. Electrochem. Soc.* **1942**, *82*, 265.

(28) Boletta, F.; Maestri, M.; Moggi, L.; Balzani, V. *J. Am. Chem. Soc.* **1973**, *95*, 7864.

(29) A similar result was observed when III was bound to sodium poly-(styrene sulfonate) in water.

(30) Caspar, J. V.; Meyer, T. J. *J. Am. Chem. Soc.* **1983**, *105*, 5583.

(31) Hauenstein, B. L.; Dressick, W. J.; Buell, S. L.; Demas, J. N.; De-Graff, B. A. *J. Am. Chem. Soc.* **1983**, *105*, 4251.
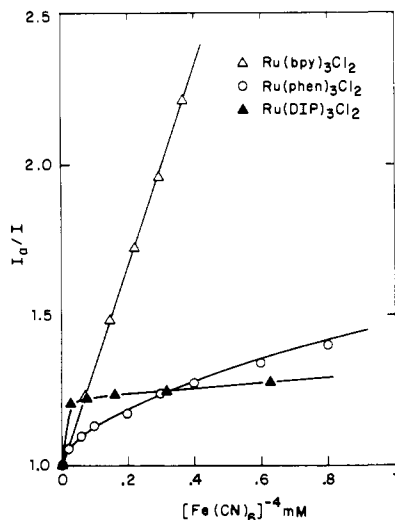
Photophysics of Ruthenium Complexes

J. Am. Chem. Soc., Vol. 107, No. 19, 1985 5521

Figure 5. Steady-state quenching of emission from ruthenium complexes in the presence of 1:40 ruthenium to DNA–phosphate in buffer solutions by potassium ferrocyanide.

Table II. Emission Lifetimes in the Presence of Added DNA at 20 °C under Air Saturation (ns)

probe	DNA/buffer	DNA/sucrose	mode of quenching by $[Fe(CN)_6]^{-4}$
I	420	773	dynamic (7×10^9 M^{-1} s^{-1})
II	733 and 2645	899 and 2000	static
III	855 and 3348	4313	static

negatively charged quencher is expected to be repelled by the negatively charged phosphate backbone, and therefore a bound ruthenium cation should be protected from quenching by an anionic quencher. On the other hand, "free" or aqueous complexes should be readily quenched by anionic quenchers. Negatively charged ferrocyanide ion was chosen for this purpose, since it quenches the emission from these three complexes with large rate constants as discussed above (Table I). Ferrocyanide ion proved to be an excellent quencher for these complexes in the presence of DNA.[32] In appropriate buffer and at a ratio of 1:40 (ruthenium to nucleotide) the emission was monitored at the respective emission maxima of I, II, and III at various concentrations of ferrocyanide, at 20 °C. The resulting Stern–Volmer plots are shown in Figure 5. The Stern–Volmer plot for I is strictly linear whereas for II and III it is drastically curved. In case of I, the linear plot gives a Stern–Volmer constant (K_{sv}) of 3.3×10^3 M^{-1} which is comparable to the K_{sv} obtained in the absence of DNA under similar conditions. The latter result is consistent with little or no binding for I to DNA. For II and III, the Stern–Volmer curves are distinctly biphasic.

These cationic complexes can potentially bind to DNA by intercalation and/or by electrostatic interactions. The former type of binding will be sensitive to ligand characteristics such as ligand planarity, the extent of aromatic π-system available for stacking interactions, and the depth the ligand can penetrate into the double helix. On the other hand, electrostatic interactions would be more sensitive to the charge of the metal ion, ligand hydrophobicity, and size of the complex ion. The bipyridyl ligand is expected to be nonplanar due to the interactions between 6 and 6' hydrogens and possesses a smaller π-system than phenanthroline or diphenylphenanthroline. Furthermore, the absence of a double bond connecting 6 and 6' carbons does not allow I to penetrate into the DNA helix as much as II and III. Finally, the overhanging 4 and 4' hydrogens of non-intercalated ligands further restrict the proximity of the ligand to the base pairs, when the complex is intercalated, significantly decreasing the available area for stacking the base pairs relative even to phenanthroline. These features disfavor intercalative binding for I to DNA relative to binding of II and III to DNA. Although the above arguments do not pertain to ionic binding, I also seems to have the lowest affinity for ionic binding perhaps somewhat surprisingly. Even though I has the same charge as II and III, it is the least hydrophobic of the complexes and is expected to have higher solubility in the aqueous environment. Model experiments,[33] employing a simple

polyelectrolyte, sodium polyacrylate, showed that I has less preference for ionic binding compared to II and III. Finally, it is noteworthy here that our measurements of binding are limited by the residence time of the metal complex on DNA. If, for example, the exchange of I between free and bound forms is very rapid compared to its luminescent lifetime, no binding would be detectable. Additionally, energy transfer between bound and free forms for I would lessen the differences in luminescence properties. The curvature and small slopes of the Stern–Volmer plots for II and III certainly are indicative of strong binding of these complexes to DNA. We interpret the initial parts of these curves to represent quenching of free aqueous ruthenium and the plateau regions to represent the insignificant quenching of the bound form by the ferrocyanide ion. The initial curved part may also include quenching due to some or more of the electrostatically bound II and III. It will be shown below from time-resolved experiments that the quenching of II and III by ferrocyanide ion is completely static. As expected, binding of II and III to DNA leads to protection from quenching by a largely negatively charged water bound quencher. This observation provides direct evidence for the binding of II and III to DNA in a form quite inaccessible to a water bound negatively charged quencher. DNA intercalation would be a binding mode consistent with this result. Additionally, the plateau regions allow a rough estimate to be made of the relative amounts of free and bound forms from eq 3 where C_b and C_f are concentrations of bound and free forms and ϕ_b and ϕ_f are

$$I_o/I_{plateau} \simeq C_f\phi_f/C_b\phi_b \qquad (3)$$

their respective quantum yields of emission. For a value of ϕ_b/ϕ_f of 1.5 for III, we estimate 73% as a lower limit for binding to DNA at a ruthenium concentration of 2.5 μM and 66% as a lower limit for the binding of II at a total ruthenium concentration of 10 μM. Hence it is clear from these simple experiments that II and III bind strongly to DNA whereas I shows little or no binding, and that the order of binding is quite consistent with ligand characteristics discussed earlier. Quenching experiments using the ferrocyanide anion greatly amplify the discrimination between bound and free forms.

Time-Resolved Emission Measurements. Binding of II and III to DNA is accompanied by remarkable increases in their emission lifetimes. These lifetimes were measured by using single photon counting techniques and are summarized in Table II. Again I served as a nonbound reference complex in these experiments. At a 1:40 ratio of ruthenium to DNA–phosphate no significant change in the clean first-order lifetime for I was observed. However, its emission lifetime could be decreased by addition of ferrocyanide, consistent with a dynamic quenching mechanism, and a rate constant of 7.1×10^9 M^{-1} s^{-1} was obtained by employing eq 1. In contrast, the emission lifetime of II and III upon binding to DNA was found to consist of two components. It is known that intercalation can cause increases in emission lifetime of ethidium bromide.[6] By analogy, the longer lived components of II and III emission are assigned to the intercalatively bound form whereas the shorter component could have contributions from ionically bound and free forms. The decay profiles for II and III are not significantly altered by 1 mM ferrocyanide, a concentration sufficient to significantly decrease the emission intensity of II and III (Figure 5). This result indicates that the quenching observed in steady-state experiments is mainly static and that the bound forms are indeed protected from the water-bound quencher. The static quenching operative under these conditions can be easily

---

(32) The millimolar ferrocyanide used in these experiments also did not appear to damage the DNA structure, based upon gel electrophoretic assays for strand scission and duplex unwinding.

(33) Work in progress in this laboratory.

Table III. Emission Polarization of I, II, and III at 20 °C

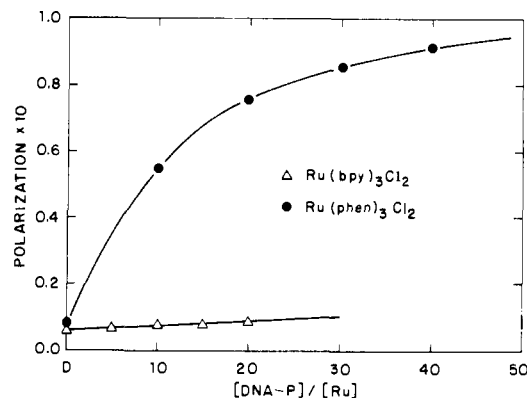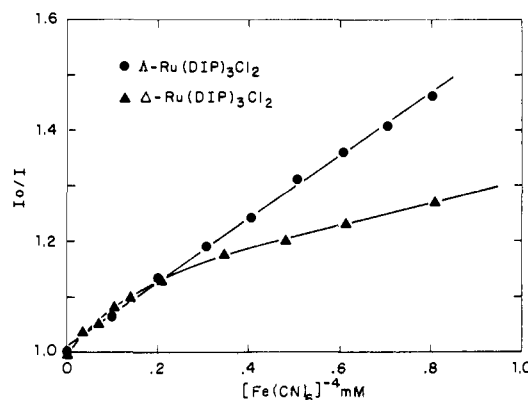| probe	λ_{exc} (nm)	glycerin	sucrose	DNA/ buffer	DNA/ sucrose
I	460	0.015	0.006	0.002	0.009
II	464	0.017	0.008	0.036	0.091
III	482	0.012	0.004	0.012	0.010
III Δ	482			0.012	
III Λ	482	0.011		0.009	
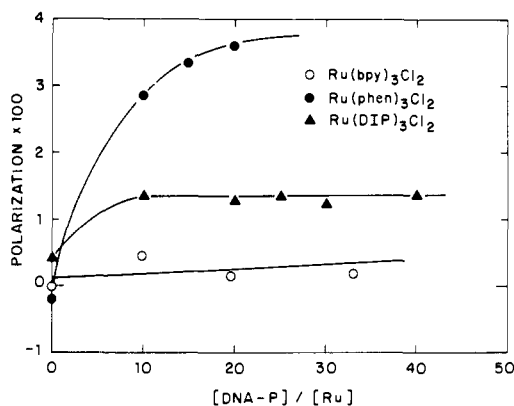
Figure 6. Emission polarization of ruthenium complexes in the presence of B-form calf thymus DNA.

Figure 7. Emission polarization of ruthenium complexes in the presence of B-form calf thymus DNA in sucrose-saturated buffer solutions.

Figure 8. Quenching of emission from enantiomers of $Ru(DIP)_3^{2+}$ in the presence of 1:40 ruthenium to DNA–phosphate by potassium ferrocyanide in buffer solutions.

understood in terms of counterion condensation in the polyion domain. The local concentrations at the polyanion are high enough for the static quenching to be dominant at these low bulk concentrations of ruthenium. These obervations further support the relative binding abilities of I, II, and III.

Emission Polarization Measurements. The electrostatic binding does not restrict the rotational freedom of the bound ion whereas intercalative binding fixes the intercalator in a specific orientation and severely restricts certain modes of rotation of the intercalator. The predicted restriction in rotation of intercalated ions can be verified by emission polarization measurements. Thus, the extent of steady-state polarization can be gauged as a measure of intercalative binding. Steady-state polarization is given by eq 4, where P is the polarization and $I_{\parallel}$ and $I_{\perp}$ are the emission intensities at parallel and perpendicular directions to the exciting

$$P = \frac{I_{\parallel} - I_{\perp}}{I_{\parallel} + I_{\perp}} \qquad (4)$$

light, respectively. The steady-state polarizations for I, II, and III have been measured under various conditions at 20 °C, and these results are given in Table III. All samples were excited at 480 nm, and the emission was observed with use of suitable filters to cut off the exciting light. The polarization of each of the complexes is nearly zero in the absence of DNA. The emission polarization for I in glycerin is in agreement with the reported value.[34] Polarizations for I, II, and III were measured at various concentrations of DNA–phosphate, and these changes are shown in Figure 6. No significant changes are observed for I whereas II and III show increases in polarization upon binding to DNA. These results provide the most direct evidence for intercalative binding of II and III to DNA by photophysical methods. It would seem surprising that polarization is observed despite the long emission lifetimes of II and III under these conditions, unless the complex was intercalated in the DNA. Thus, the degree of polarization is a measure of DNA motion and not that of the rigidly intercalated complex. Indeed the polarization for II was further enhanced in a viscous saturated sucrose solution. The DNA motions are expected to slow down under these conditions leading to a further increase in polarization for the intercalators. No such effect was found for I in viscous sucrose solution. These changes upon binding to DNA are shown in Figure 7 for I and II. Thus

polarization measurements provide compelling evidence for intercalative binding of II to DNA. III does not seem to bind under these conditions and is evidently solubilized by the sucrose solution.

Enantiomeric Selectivity for Binding. Strong enantiomeric selectivity may be observed for the binding of chiral metal complexes to DNA. $Ru(DIP)_3^{2+}$ provides an excellent example. The large expanse of its left-handed non-intercalative ligands precludes insertion into a right-handed B-DNA helix.[16] Large changes in emission intensities were observed[35] when DNA solutions were added to the Δ and Λ isomers of III, indicating that both bind to DNA. Although both Δ and Λ forms bind to B-DNA, the nature of binding was found to be different for each of these two forms. When the emission from each of these isomers was quenched upon binding to DNA, using ferrocyanide as the quencher, a marked difference between Δ and Λ forms became apparent (Figure 8). The quenching plot for Δ is curved downward, as it is for the racemic form, whereas a linear plot was obtained for the Λ isomer. This result is consistent with the Δ isomer being bound to DNA by intercalation and thereby being inaccessible to quenching by the water-bound ferrocyanide. Linear quenching plots were oberved with either Δ or Λ isomer in the absence of DNA. The striking linearity of quenching of emission from the Λ isomer in the presence of DNA indicates that it is bound only electrostatically and not by intercalation and is relatively accessible to quenching by ferrocyanide. It may be further pointed out that the K_{sv} for the Λ isomer is 540 M^{-1} as against a value of 440 M^{-1} for racemic III in the absence of DNA. While only one binding mode is detectable for Λ-$Ru(DIP)_3^{2+}$, the Δ isomer binds in two forms, electrostatically and by intercalation. The intercalative mode is therefore stereoselective for Δ-Ru-
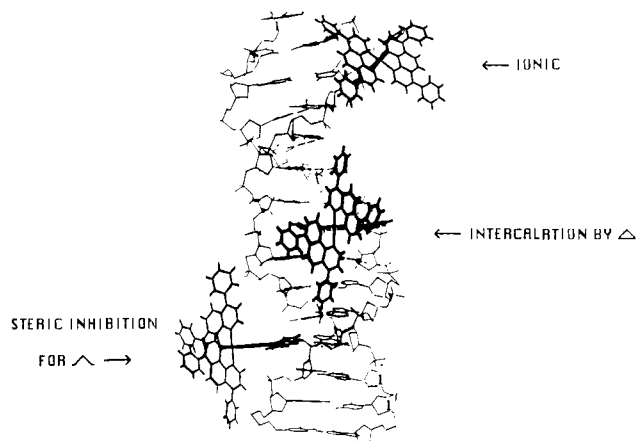
---

(34) Fujita, I.; Kobayashi, H. *Inorg. Chem.* **1973**, *12*, 2758.

Figure 9. Enantiomeric selectivity for Ru(DIP)₃²⁺ in binding to B-DNA. Top: Ionic binding of Λ isomer to the sugar–phosphate backbone. Middle: Intercalation of Δ isomer into the double helix. Bottom: Steric inhibition of intercalation of Λ isomer into the helix.

(DIP)₃²⁺. This conclusion is further supported by polarization measurements in which higher values for polarization were observed for the Δ isomer than for the Λ isomer upon binding to DNA (Table III). It is clear from these experiments then that significant enantiomeric discrimination of Δ relative to Λ occurs in binding to B-DNA.

The enantiomeric selectivity governing binding of Ru(DIP)₃²⁺ enantiomers to B-DNA is best understood in terms of the intercalative model depicted in Figure 9. When intercalated into the right-handed helix, the disposition of non-intercalated ligands of the Δ isomers matches the helical asymmetry of the right-handed DNA groove. For the Λ isomer the orientation of the ligand opposes the helical groove, and steric constraints completely preclude binding of Λ-Ru(DIP)₃²⁺, with the large bulk of its non-intercalated ligands, within the helix. The Λ isomer may, however, bind electrostatically to the DNA helix, and in Figure 9, for the Λ isomer, such an electrostatic association, or ion condensation, is depicted. This binding mode, altering the surrounding water structure of the metal, is also likely to alter its emission properties. The increase in excited-state lifetimes might be expected to be smaller than that for intercalative binding, however. Quenching of condensed ruthenium cations by ferrocyanide would also likely be greater than that for intercalatively

Table IV. Binding Characteristics of Ruthenium Complexes with DNA

	methods of analysis			mode of binding	
probe	emission enhancement	[Fe(CN)₆]⁴⁻ quenching	steady-state polarization	inter-calation	ionic binding
I	none	linear	none	–	– (?)
II	yes	biphasic	yes	+	+
III Δ	yes	biphasic	yes	+	+
III Λ	yes	linear	(no)	–	+

bound cations. The loosely held, ionically bound species, which may even be exchanging rapidly with free ruthenium, are significantly more accessible to the anionic quencher than the intercalatively bound species. Emission polarization results are consistent with this model as well, since rigidly bound intercalation of the Δ isomer would give rise to a polarization higher than that for the electrostatically bound Λ isomer.

Conclusion

Modes of binding each of these metal complexes to the DNA helix may be distinguished readily by taking advantage of the different photophysical properties of ruthenium(II). A summary of these modes and the methods of analysis used for these determinations are given in Table IV. It is our conclusion that binding of Ru(bpy)₃²⁺ to DNA is negligible, either by intercalation or by electrostatic interactions. In contrast both Ru(phen)₃²⁺ and Ru(DIP)₃²⁺ show a strong affinity for DNA. Here two modes of binding are evident and are assigned to intercalation and electrostatic association. Significant enantiomeric selectivity in intercalation is found for Ru(DIP)₃²⁺, and it is the Δ isomer that binds preferentially by intercalation. For these complexes, the emission lifetimes are increased significantly upon binding to DNA, just as are the emission intensities. With use of ferrocyanide anion, the quenching of emission from these probes in the presence of DNA can clearly distinguish between bound and free forms and indeed between the rigid intercalatively bound form and the loose electrostatic component. Emission polarization provides additional evidence in support of these different binding modes.
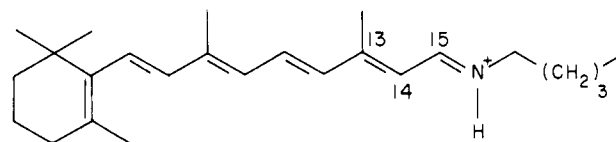
Communications to the Editor

Dynamic Cis–Trans Isomerization of Retinal in Dark-Adapted Bacteriorhodopsin

Stanley Seltzer* and Ron Zuckermann†

*Chemistry Department, Brookhaven National Laboratory
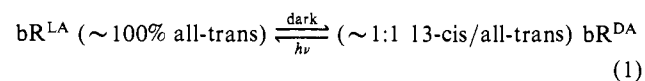Upton, New York 11973*

Received January 21, 1985

The purple membrane, the light-driven proton pump of *Halobacterium halobium*, contains a proteinic pigment, bacteriorhodopsin (bR), present in trimeric form, wherein the retinal is bound to lysine 216 of bR via a protonated Schiff base I.[1] Retinal,

(1) For a recent review, see: Stoeckenius, W.; Bogomolni, R. A. *Annu. Rev. Biochem.* **1982**, *52*, 587–616.

I

which in light-adapted bR (bR^LA) is ∼100% all-trans, isomerizes in the dark to a resting, dark-adapted form, bR^DA, containing a ∼1:1 bound mixture of *all-trans-* and 13-*cis*-retinal (eq 1). It

$$\text{bR}^{\text{LA}}\ (\sim 100\%\ \text{all-trans}) \underset{h\nu}{\overset{\text{dark}}{\rightleftharpoons}} (\sim 1{:}1\ \text{13-cis/all-trans})\ \text{bR}^{\text{DA}}$$

(1)

has been shown recently that two adjacent double bonds cis–trans isomerize in reaction 1. The chromophore of bR^LA is protonated 13-*trans*,15-*anti*-retinylidene Schiff base (I); in bR^DA half the